Heritage Science

RESEARCH

Open Access

Risk of fracture in massive cultural objects made of lime wood: a case study of Veit Stoss' altarpiece

Magdalena Soboń[1*] and Łukasz Bratasz[1]

Abstract

Massive cultural objects made of wood are often situated in historic interiors in which they experience uncontrolled dynamic variations of relative humidity (RH). Although the objects usually have acclimatized to the natural climate variability, preventing risks related to any kind of modification of their environment requires an understanding of the object's response to the expected changes. In the present study, an analysis of the risk of cracking related to continuous or intermittent heating, or the transfer to hypothetically ideal conditions in a conservation studio was performed for the case of elements of Veit Stoss' altarpiece (1477–1489) preserved in St. Mary's Basilica in Krakow, Poland. Massive sculptures carved in lime wood and approximately one meter in diameter were analysed. The study aimed at determining safe margins of environment modifications that would not cause propagation of cracks that are known to have accumulated in wood during centuries of the altarpiece's existence. The mechanical properties of lime wood were determined experimentally to feed the numerical model. The energy release rates around the tips of cracks of various depths in a wooden sculpture were calculated using the finite element analysis and compared with the critical value of the parameter triggering the fracture propagation in the material, derived from the fracture energy measurement. It was shown that the church interior housing the altarpiece can be heated to 11 °C during the cold season to provide human comfort. The allowable duration of intermittent heating events to more comfortable 18 °C that would induce drops in RH of up to 40% was assessed as 12 h. The study demonstrated that moving the sculptures to the conservation studio would have to be done with extreme caution as it would be connected with risks depending on the depth of existing cracks and the duration of the RH change.

Keywords Wooden sculptures, Lime wood, Veit Stoss' altarpiece, Risk of fracture, Indoor environment, Preservation of cultural heritage, Finite element method, Numerical modelling

Introduction

Among the wooden art in Central Europe, a great proportion is made of lime wood (*Tilia sp.*). Lime wood was favoured by artisans and sculptors due to the combination of desired features: light colour, an indistinctive pattern of growth rings, and ease of processing. The large main altar in the St. Mary's Basilica in Krakow, which is the focus of this study, was also carved in lime wood in 1477–89 by Veit Stoss, a sculptor from Nürnberg. The 13 m high, polychromed and gilded altarpiece is equipped with two movable wings which can be opened or closed on the central part with sculptures and a further pair of fixed wings (Fig. 1). Sculptures are up to one metre in diameter. The backs of large sculptures were concave cut hollow to reduce their weight as well as their vulnerability to cracking.

As wood is a hygroscopic material, variations in its moisture content (MC) result in changes in its

*Correspondence:
Magdalena Soboń
magdalena.sobon@ikifp.edu.pl
[1] Jerzy Haber Institute of Catalysis and Surface Chemistry, Polish Academy of Sciences, 30-239 Krakow, Poland

Fig. 1 Veit Stoss, the main altar in St. Mary's Basilica in Krakow, 1477–1489, painted lime wood. Photo: Zygmunt Put (Image reproduced under Wikimedia Commons public domain licence, https://commons.wikimedia.org/wiki/File:Church_of_Our_Lady_Assumed_into_Heaven,_St._Mary%27s_(Main)_Altar_(1489_by_Veit_Stoss),_5_Mariacki_square,_Old_Town,_Kraków,_Poland.jpg

dimensions, which engenders a stress field in the material if the (free) movement is restrained. The source of the restraint can be external, resulting from the excessively rigid construction restricting movement, or by assembling wood elements with the different mutual orientations of their fibre direction, or internal due to the mismatch of dimensional response in the different anatomical directions of wood or a gradient of MC when the exterior part of the wood responds more quickly than the interior to a change in ambient relative humidity (RH). In general, the moisture-related dimensional response is significantly larger in the direction perpendicular to the grain than in the parallel direction, which for practical applications can be considered negligible. From among the two directions perpendicular to the grain, dimensional response in the tangential direction approximately doubles this in the radial one. Thermal expansion or contraction has a minor effect on the overall dimensional changes of wood objects as compared with its response to moisture. Therefore, the contribution of RH variations to stress development and resulting damage is significantly larger compared to the contribution of temperature variations [1–5].

As detailed in our initial publication [6], long-existing awareness of the correlation between climate instability and the condition of wooden heritage objects was a motivation for adopting environmental specifications for the preservation of cultural heritage objects in museums. Foundations for the evidence-based environmental specifications were laid by Mecklenburg [2, 3, 7, 8], who quantified the key mechanical and moisture-related parameters—stiffness, strength, strain at break, yield point, and hygroscopic expansion coefficients—for materials relevant to cultural heritage including wood. However, the majority of the predictive models [8] assume full equilibrium of the object with the surrounding environment or evaluate the global dimensional response of objects neglecting local stress fields [9], which reflects well risks caused by slow RH variations. In consequence, most environmental specifications to preserve valuable collections do not take into account the environmental specificity of religious buildings and historic houses. Typically, such buildings are characterized by high variability of environmental conditions occurring over short times either due to the use of intermittent heating to provide thermal comfort during religious services, or cultural and commercial events, or because of a limited potential of historical buildings to control the indoor environment. Such dynamic environmental variations are rare in modern buildings housing collections due to their different construction, function, and pattern of use, contributing, generally, to a much higher potential for climate control. The most recent and globally influential guidelines for museums, galleries, libraries, and archives provided by the American Society of Heating, Refrigeration and Air-conditioning Engineers ASHRAE [10] is a good example. The guidelines, explicitly assume that variations shorter than the response time of the object are safe. This might be true for several categories of objects but is not true for all, including massive wooden sculptures. For a dynamic RH change, MC differs in the outer and internal parts of massive objects owing to their long response time, which results in different dimensional responses of the outer and inner parts. The magnitude of moisture gradient is higher when a sculpture is not painted or is covered with ground and paints permeable to water vapour like animal glue-based grounds and tempera paints. In turn, oil paints or gilding act as water vapour barriers which reduce the influence of environmental variations on the outer zone of the wood [11].

Jakieła et al. were the first to study the risk of damage for massive objects made of lime wood by modelling stress formation in a cylinder subjected to a step RH variation using the finite element method [12]. Their approach was based on classical mechanics and delivered information about the stress levels varying across the cylinder. Using the information, the authors evaluated conditions under which the stress levels become critical.

Fracture mechanics has been applied to study crack development in wood since the 1960s [13]. The numerical predictions of fracture phenomena have been possible due to the development of Rice's theory of *J*-integral [14] and the first successful attempt to extend it to wood was undertaken by Yeh and Schniewind [15]. Also, the analysis of local stress fields can be successfully applied to numerically predict cracking in wood under both thermally- and moisture-induced loads as shown by Luimes and Suiker [1]. A criterion of maximum tensile strength was used to predict local crack nucleation in oak wood cabinet door panels and crack propagation was modelled using the traction–separation law incorporated in the interface-damage model. Similarly, Gebhardt and Kaliske [16] proposed an approach based on an extended finite element method for modelling fracture in wood where stress-based criterion allowed the location and orientation of the crack growth to be identified, whereas the anisotropic traction–separation law at the crack faces informed actual fracture behaviour. Chen et al. [17] analysed the model that already contained a pre-crack and used the maximum tangential stress as the indicator of crack growth direction in timber cross-sections subjected to drying. Further fracture was modelled with the virtual crack closure technique, which allowed the components of energy release rate (G) to be calculated and compared with the critical level G_c, a criterion for crack propagation.

Among several fracture mechanics methods, one of the most popular is the *J*-integral theory to approach the problem of climate-induced wood cracking [18–20]. Soboń and Bratasz [6] used the *J*-integral method to analyse *G*, and more specifically energy release rate in the opening mode G_I, around the tip of cracks of various depths in the wooden sculpture made of pine and exposed to step and sinusoidal RH variations. By comparison of the G_I value calculated for changes of various amplitude, duration, or period with critical energy release rate G_{Ic}, the authors showed that step variations of amplitude lower than 19% RH were safe for the sculpture. Similarly, a change shorter than 48 h would not cause crack propagation. They also demonstrated that sinusoidal variations generated a larger risk than step variations due to the shift of the long-term MC average caused by the increase of diffusion coefficient and the derivative of sorption isotherm with MC. It was shown that the maximum value of G_I was generated by a sinusoidal variation of half a year for cracks 15 mm deep. The minimal amplitude that could induce further crack propagation was 16% RH.

The adequacy of G_c as a damage criterion is an important issue raised in the literature on wood fracture. The specific fracture energy G_f was proposed as a more adequate parameter since it accounts for the non-linear elastic fracture behaviour of wood [21]. G_f characterizes total energy dissipated by crack initiation and its propagation, and its value is larger than G_c due to the occurrence of energy-consuming processes like the formation of microcracks in the process zone [22]. G_f can be determined in mechanical tests—three-point bending [23] or wedge-splitting developed particularly for this purpose by Stanzl-Tschegg et al. [22]. In both mentioned methods, a pre-cracked specimen is subjected to loading in mode I, and force and displacement are measured during the crack growth. G_f, as other mechanical parameters of wood, varies with the material's MC [24] and strongly depends on its orthotropic properties [25, 26]. Experimental values of G_f of various wood species can be found in literature as well as their dependence on the crack-propagation system and MC [21, 24, 27], however, to the authors' knowledge, this parameter has not yet been measured, and published for lime wood.

The main aim of this paper is to apply the methodology presented in [6] to risk analysis of real objects, in this case, Veit Stoss' sculptures carved in lime wood, exposed to natural RH variations and formulate recommendations for climate control during religious and cultural events organized in the basilica in which they are preserved. However, the barrier to reaching this goal was the lack of relevant mechanical properties for lime wood. Due to lime wood softness and limited durability, this wood species is not suitable for construction and engineering purposes and as a result, the information about mechanical parameters available in the literature is very limited. The moisture sorption data were published by Majka and Olek [28] and Popescu and Hill [29]. The isotherms of moisture-induced dimensional change, moduli of elasticity, and strain at break were published by Rachwał et al. [9], and Jakieła et al. [12]. The analysed gap in knowledge was partially filled by a very recent work by Konopka et al. [30], in which data regarding sorption, dimensional change, and mechanical parameters of lime wood (*Tilia cordata*) tested under compression and tension were provided with their relation to the RH level.

Materials and methods

Samples preparation

Logs of seasoned lime wood were acquired from three different sources. Owing to a very limited supply of the material, it was impossible to acquire wood of uniform quality, and its different levels were assigned to the logs by visual inspection, which later was confirmed by mechanical test results. Log no. 1 was donated by a professional restorer after being seasoned for more than 10 years in a conservation studio. Log no. 2 was purchased from a local amateur sculptor. The wood was air-seasoned for eight years, unprotected from weather conditions, due to which some discolorations in the cross-section were observed. The distribution of the growth rings' distance was uneven. Log no. 3 was stored in the laboratory after previous projects. It was characterized by a very dense pattern of growth rings and their flat curvature due to the large diameter of the tree.

Logs were machined to the desired shape and orientation—properties in the tangential (T) and radial (R) anatomical directions of wood were of interest in this study. The specimens were stored in four plastic airtight enclosures with a seal placed between the lid and the container. Inside each enclosure, a 1.5 l plastic container with a perforated lid was filled with ca. 1 l of the saturated salt solution maintaining the desired RH [31] monitored using a HOBO MX1101 T/RH data logger from the Onset Computer Corporation. An electrical fan (5 × 5 cm) was placed on the lid to improve the air circulation in the enclosure. Specimens were kept in the enclosures until they achieved equilibrium moisture content (EMC) specific for each RH level. Equilibration was assessed by weighing the specimens on the precise laboratory balance every 4-7 days until the weight of the specimen remained unchanged. After the mechanical experiments, the specimens were dried in an oven and EMC was calculated as the mass of water per mass of dry wood expressed in percent.

Before placing the specimens in the enclosures with the two highest RH levels, their surfaces were brushed with a solution of Preventol RI 50 from Kremer Pigmente GmbH in distilled water at 12% volume concentration to limit the risk of mould growth and left in a fume cupboard for 24 hours. After the mass of specimens stabilized, the ones exposed to the highest RH level were covered with two layers of wax paste for wood (a mixture of beeswax and carnauba wax from Colorit, ICA Polska Sp. z o.o.) on their TR surfaces—perpendicular to the grain—to prevent moisture exchange with the air during the mechanical tests in the laboratory. Then the specimens were placed again in the enclosures for several days for the final stabilization. Other specimens were not protected from unwanted moisture exchange as the RH level in the laboratory during mechanical tests was approximately corresponding to the stabilisation level.

Mechanical experiments

Mechanical experiments were conducted at room temperature and RH approximately the same as in the enclosure, where the specimen was kept. Fracture toughness experiments with specimens from the enclosures with two highest RH levels were the exception. They were performed at RH between 60 and 70% as humidification of the room was insufficient. During the tensile tests, these specimens were contained in an airtight compartment of the testing equipment and ventilated with the air from an environmental chamber POL-EKO KK 700 Smart Pro to maintain the high RH levels required. Covering specimens with wax as well as controlling RH in the laboratory ensured that even during the longest experiment the change of specimen's EMC measured by weight loss was less than 1.5%. Seven or eight and between two and five tangentially or radially cut specimens, respectively, were tested in the tensile tests, whereas three to five specimens were tested in the wedge-splitting tests at each EMC level.

Moduli of elasticity, Poisson's ratios, and strains at break were determined in the tensile tests using UTM from Hegewald & Peschke MPT GmbH (Nossen, Germany) equipped with a 10 kN load cell. The modulus in the radial or tangential directions and the associated Poisson's ratio were measured simultaneously in one experiment along with the strain at break. A dog-bone-shaped specimen of dimensions 9 × 11 × 50 mm of the thinnest part, similar to one described in [32], was mounted in the clamps and subjected to tension until break. The speed of the crosshead was 0.2 mm/min. The deformation in the direction perpendicular to tension was measured with a mechanical extensometer from Hegewald-Peschke of an accuracy of 0.2 µm, while in the direction parallel to tension the deformation was measured using an optical extensometer ONE of accuracy 2 µm from the same manufacturer as UTM.

Fracture energy was determined according to the splitting method [22]. A steel wedge with a 13-degree angle was mounted in the clamps of a Zwick/Roell Z2.5 TN Universal Testing Machine with a 2.5 kN load cell Xforce P grade 1 accuracy. When the clamps approach each other, the wedge exerts force on a specimen leading to the crack opening. The geometry of the specimen is depicted in Fig. 2 and the dimensions in mm are: W = 100, T = 30, a = 46, L = 84, H = 130. Crack propagation in the TR system was investigated with the tangential plane T perpendicular to the crack and the crack growth in the radial direction R. A starter notch was machined to 42 mm of depth and a final extension of 4 mm was made using a razor blade.

Vertical force is transformed into horizontal one through the rollers mounted on the specimen's sides at the axes of the rollers. The speed of the crosshead was 0.2 mm/min as in the tensile test. The displacement was measured using a video extensometer (videoXtens 1C/1H, Zwick-Roell) synchronized with the UTM from a distance of 785-800 mm. The field of view of the video extensometer was ca. 145 × 115 mm and its accuracy was 1 µm. For each measurement, a video was recorded. Since it was impossible to break the specimen completely, fracture energy was determined as the area under the horizontal force component – displacement curve minus the area under the straight line joining the starting point of the measurement with the final one on the force-displacement graph, and the difference was divided by the fractured surface. All data processing was done using the OriginPro ® 2020 software and Gadget: Integration tool.

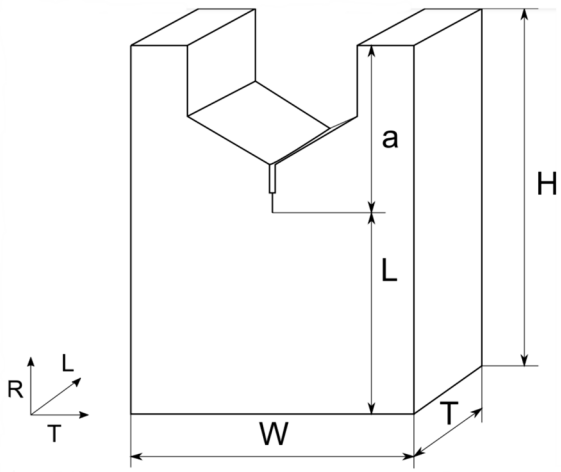

Fig. 2 Geometry of a specimen tested in the wedge-splitting experiment after [22]

To obtain the fractured surface, the specimen's thickness T was multiplied by the average crack length measured using the ImageJ 1.53k software [33] on the final frame of the recorded video. The error linked with the crack length was substantial due to the tortuous shape of the crack walls.

Model

The model of a sculpture developed after [6] is shown in Fig. 3. As indicated in the introduction, the backs of large sculptures of the altarpiece were concave cut hollow which has reduced stress fields engendered in the structures by environmental variations and their susceptibility to cracking. However, in this study, a wooden sculpture was represented by a full wooden cylinder with the *z*-axis coinciding with the central axis of the tree trunk to model the worst-case condition for the stress increase and crack development.

The important modifications compared to the previous approach described in [6] was, firstly, the use of lime wood (*Tilia sp.*). Secondly, the diameter of the modelled sculpture was increased to 1 m to account for the significant size of the most prominent sculptures in the Veit Stoss' altar. The mesh was adapted as in Fig. 3 and the number of domain mesh elements was ca. 43,000. The remaining model assumptions including mathematical modelling and equations introduced for fracture mechanics calculations remained unchanged. The necessary alterations included the following model's parameters: moisture sorption isotherm, moduli of elasticity in the T and R directions, shear modulus in the TR direction, Poisson's ratio values, hygroscopic expansion coefficients, and wood density. Since the mechanical properties of wood strongly depend on the wood's EMC, this fact was accounted for both in the laboratory experiments and the model.

Water vapour adsorption and desorption isotherms for lime wood measured by Bratasz et al. [34] were used in this work to determine scanning isotherm using the procedure described in [10], based on the approach proposed by Mualem [35].To correct the printing error in the parameters of the equation describing the desorption branch of the isotherm in [34], new parameters were obtained by fitting the equation to the original experimental data. The density of lime wood was taken from [10]. The hygroscopic dimensional change corresponding to the MC values described by the scanning isotherm was interpreted by fitting the sigmoidal function to the experimental data obtained by Bratasz et al. [36] relating the hygroscopic dimensional change α to MC. Equilibrium moisture contents EMC, moduli of elasticity E, Poisson's ratios ν, density ρ, hygroscopic dimensional changes α, diffusion coefficient D, surface emission coefficient h' of lime wood and their relationships with RH,

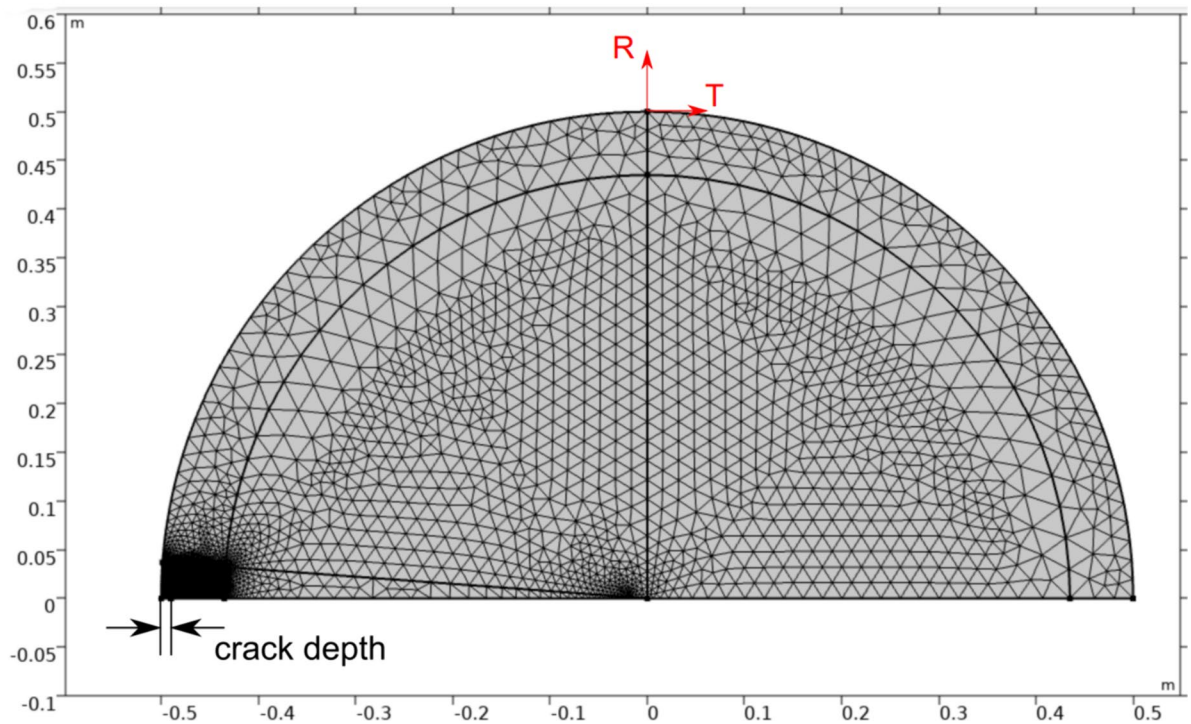

Fig. 3 Model of a sculpture after [6] with the diameter 1 m and the adapted mesh

Table 1 Parameters of lime wood and their relationships with RH or MC used in the modelling

Property	Value or formula	Units	Source
EMC	$-0.21+0.38RH-0.01RH^2+2.91RH^3\times10^{-4}-3.35RH^4\times10^{-6}+1.6RH^5\times10^{-8}$	%	Function fitted to the data from [34]
E_R	$[-3.36\exp(RH/18.52)+1026.66]\times10^6$	Pa	Own measurements
E_T	$[-8.48\exp(RH/26.88)+577.49]\times10^6$		
G_{RT}	$[E_R(RH)+E_T(RH)]/[4+2(\nu_{TR}+\nu_{RT})]$	Pa	Formula adopted after [6]
ν_{RT}	$\nu_{TR}E_R(RH)/E_T(RH)$	–	Formula adopted after [6]
ν_{TR}	0.322	–	Own measurements
ρ	500	Kg/m^3	[9]
a_T	$10.59\frac{MC^{1.51}}{82.73+MC^{1.51}}$	–	Function fitted to the data from [36]
a_R	$5.15\frac{MC^{1.51}}{56.36+MC^{1.51}}$		
D	$1.44RH^{1.8449}\exp(-5280/T[K])\times10^{-7}$	Kg/msPa	[6]
h'	3×10^{-8}	Kg/m^2sPa	[6]

Table 2 Equilibrium moisture contents EMC in lime wood

RH level measured in the enclosure (%)	Average EMC value measured (%)	RH level calculated from the EMC – RH relationship used in this study (%)
38	6.6	45
60	8.9	64
81	12.9	83
> 95%	19.2	94

MC, or temperature (T) used in the modelling are given in Table 1.

Results and discussion

Equilibrium moisture contents

Average EMC values determined in specimens stored prior to the mechanical tests in the enclosures, in which different RH levels were maintained, are listed in Table 2. As EMC depends on the sequence of processes of adsorption and desorption that the specimen experienced in the past, the relationship between EMC and RH assumed in this study and provided in Table 1 was used to calculate RH values corresponding to the EMC determined. They are listed in the last column of Table 2.

Tensile properties

The load versus extensions data measured in the tensile tests were recalculated to true stress and true strain The moduli of elasticity were determined as a linear fit to the portion of the true stress versus true strain curve between 0 and 0.0025 of true axial strain. Poisson's ratios were deduced as the negative ratio of true transverse strain to true axial strain and the values were determined from a linear fit to the portion of the stress-strain curve between 0.0015 and 0.0025 of true axial strain. The

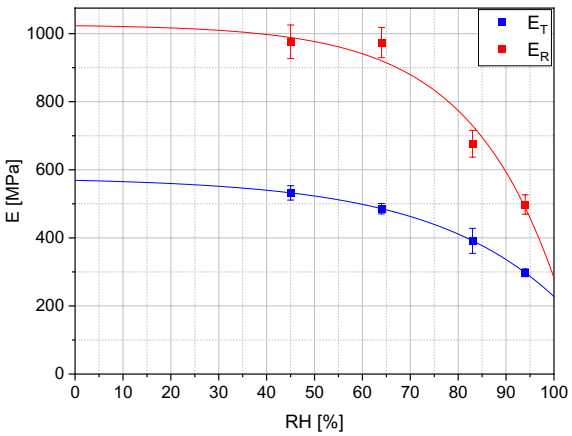

Fig. 4 Average values of the moduli of elasticity measured in the tangential and radial directions of lime wood with fitted exponential functions

average value of the modulus of elasticity and its standard deviation were determined for each RH corresponding to the average EMC listed in the last column in Table 2. The dependence of the modulus of elasticity in the T and R directions on RH is depicted in Fig. 4. The modulus decreases with increasing RH. Exponential functions were fitted to the data points and used in the modelling (Table 2). The values determined agree well with the ones obtained by Konopka et al. [30].

Average values of the Poisson's ratios and their standard deviations were determined for the same RH levels. The average values of ν_{TR} and ν_{RT} and their dependence on RH are depicted in Fig. 5. Contrary to the modulus of elasticity, ν_{TR} is independent of RH. Therefore, in the modelling, a constant value of $\nu_{TR} = 0.322$ calculated as the weighted average of points depicted in Fig. 5 was used. The authors of [30] did not present the measured

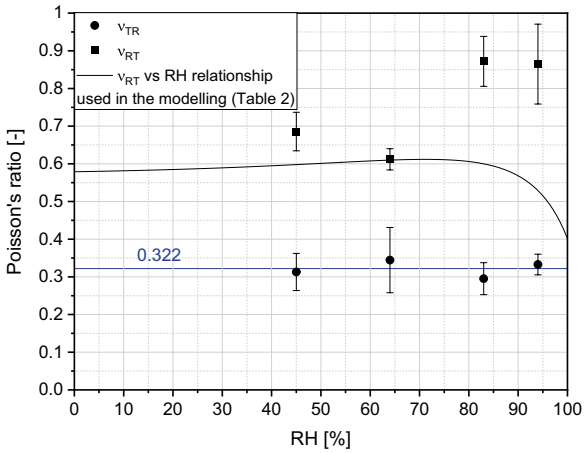

Fig. 5 Poisson's ratios ν_{TR} and ν_{RT} determined for lime wood and the average value of ν_{TR} used in the modelling

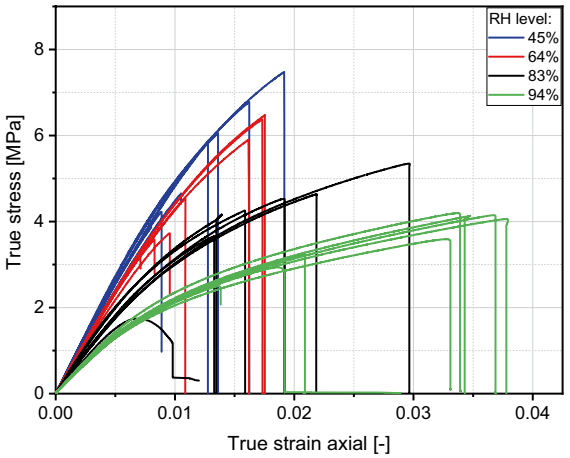

Fig. 7 True stress versus true axial strain curves for all lime wood specimens cut in the tangential direction T

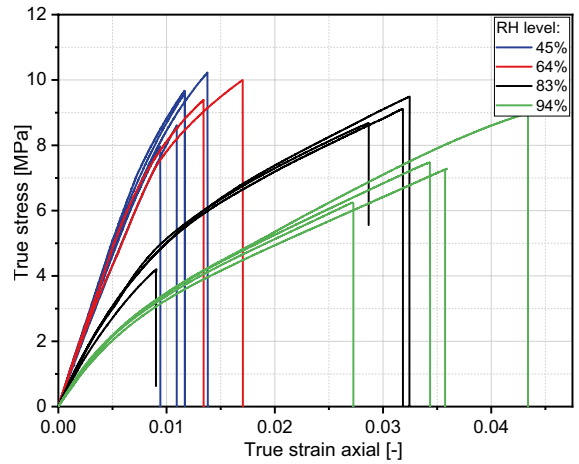

Fig. 6 True stress versus true axial strain curves for all lime wood specimens cut in the radial direction R

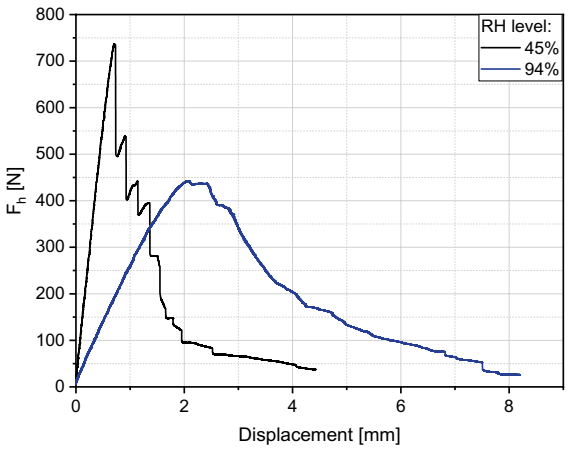

Fig. 8 Plots of horizontal force component F_h versus displacement recorded in the mode I wedge-splitting experiments of lime wood specimens in the TR crack propagation system equilibrated at 94% and 45% RH

value of ν_{TR} but ν_{RT} measured in their experiment is almost identical to the value in this work. The moduli of elasticity and Poisson's ratios determined in this work were used in the modelling to ensure coherence with the fracture energy values.

Each tensile test was performed until the break of the specimen to determine the value of strain at break. All true stress versus true strain curves for the specimens cut in the R and T directions are presented in Figs. 6 and 7, respectively. The dependence of the strain at break on RH is evident and, within the experimental error, there was no difference between the two anatomical directions. The variability of curves measured at the same RH level has its origin in specimens being cut from various trunks and it reflects the natural variability of wood.

Fracture energy

Figure 8 illustrates typical plots of horizontal force component F_h versus displacement for high and relatively low RH levels recorded in the wedge-splitting experiments used for calculations of G_f. A large drop in F_h is observed in the plot obtained at low RH (black line) in contrast to a monotonic decrease of the parameter at high RH conditions (blue line). The experiment was stopped before the specimen broke completely when the force dropped to ca. 5% of the maximum value.

While the plot obtained for high RH indicates a stable crack growth, the plot for dry conditions indicates the so-called *snap-back behaviour* and leads to an overestimation of the fracture energy calculated from the area under

the curve since the displacement-controlled experiment cannot follow the decrease in the deflection occurring with the dynamic drop in load [23]. It was shown in the same study that the correct fracture energy values need to be derived from the finite-element modelling. Such correction was introduced in this study as described below. The uncorrected fracture energy values as determined in the wedge-splitting experiments are presented in Fig. 9 for each tested specimen to reflect the scattering of the results between specimens machined from different wood logs. The error bar of each G_f value was calculated using a propagation of uncertainty. The uncertainty of determination of the crack length due to the tortuous shape of the crack walls was the predominant source of the uncertainty of each measurement. The diamond-shaped points are the weighted average G_f with error bars indicating the error of the weighted average calculated for each RH value related to specific EMC values as in the previous paragraphs. The average G_f slightly increases with RH from 350 N/m up to 750 N/m at 83% and then decreases to 570 N/m at RH = 94%. However, the reduction is within the experimental uncertainty.

While G_f describes the whole fracturing process, G_{Ic} is the parameter that, in the opening mode, indicates the onset of crack growth in the material. Vasic and Stanzl-Tschegg determined G_f experimentally with the wedge-splitting method and G_{Ic} with the finite element method for four wood species and at four RH levels [27]. From their data, the lowest ratio of G_{Ic} to G_f was 0.60 and this value was adopted as representing the worst-case—an approach frequently used in safety analysis. By taking the G_f value of 350 N/m determined in this study at 45% RH and multiplying it by 0.60, the value of 210 N/m is obtained which can be rounded down to 200 N/m. We refer to that value as G_{Ic} for lime wood in the analysis of modelling results presented below.

Modelling results

Microclimate in St. Mary's Basilica in Kraków in the environment of Veit Stoss' altarpiece was measured for a year between May 5, 2014 and May 5, 2015. A slowly varying component of RH was extracted using a low-frequency filter with the cut-off duration frequency of 0.03 Hz leaving only durations longer than 36 h. The data were then interpolated to obtain 100 data points for the simulation. The recorded RH and its slow component are shown in Fig. 10. The average RH was 59% while the slow variation changed between a maximum of 66% and a minimum of 49%. The temperature records were processed in the same way.

The slowly varying component of the climate interpolated to 100 points was used to determine the moisture profile along the radius of the sculpture. To achieve the equilibrated profile, the calculations were repeated 50 times. Figure 11 shows G_I induced in a modelled wooden sculpture 1 m in diameter by the microclimate variations in the sculpture's environment over one year. Initially, three crack depths: 5, 15, and 30 mm were selected, corresponding to the maximum values of G_I obtained in the simulations of sinusoidal variations of periods of 7, 90, and 365 days, respectively. Those variations representing typical climatic scenarios were simulated as in [6] and the results are provided in the supplementary material. Subsequently, two further crack depths for which the G_I value was close to the maximal one: 10 and 12.5 mm were also considered.

The maximum G_I value was obtained for crack depths of 12.5 and 15 mm and it corresponded to the drop in RH

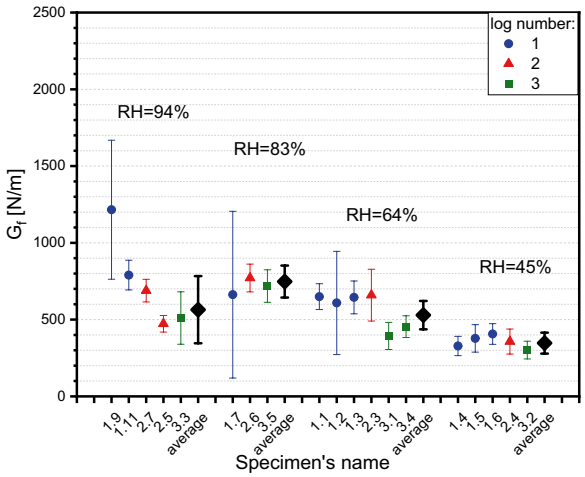

Fig. 9 G_f values obtained for lime wood in the mode I wedge-splitting experiments in the TR crack propagation system at various RH levels

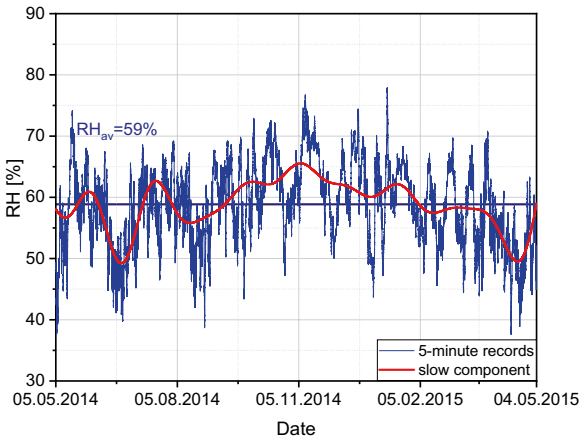

Fig. 10 Indoor RH in the environment of Veit Stoss' altarpiece recorded every five minutes and its slow component for a full year

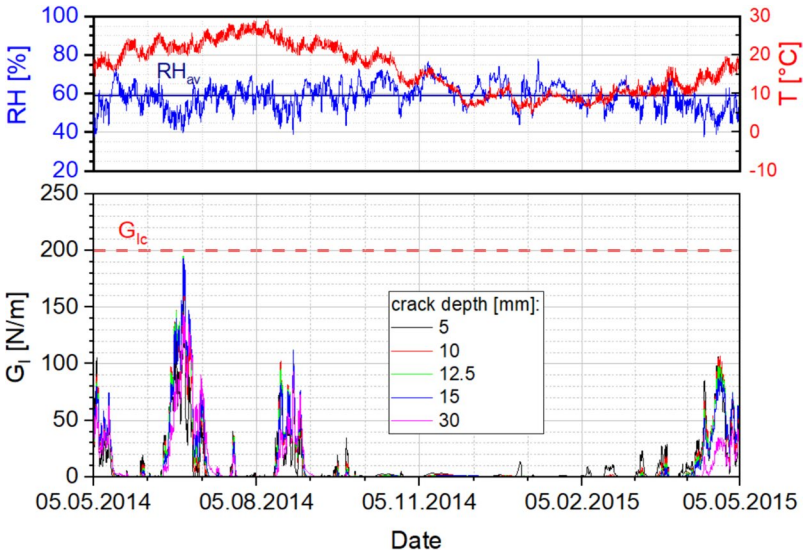

Fig. 11 Effect of the microclimate in St. Mary's Basilica on the G_I values in a sculpture modelled

on June 23. Interestingly, a similar drop in RH on April 20, resulted in G_I almost two times smaller than the drop on June 23. The reason for the observed difference is lower indoor temperature in April than in June—approximately 10 and 20 °C, respectively, which resulted in two times lower diffusion coefficient D and thus slower drying of the sculpture in April. For all the simulated crack depths, the obtained G_I values were below the critical level, which indicates no risk of further fracture in the sculptures in the current environmental conditions. This result is in agreement with the condition survey performed by the conservation team restoring the altarpiece which revealed no environmentally induced new damage in the sculptures. As the demand for human comfort during services and cultural events is increasing, a hypothetical scenario of an increase in temperature during the cold season in the basilica to reduce the current drops even to 4 °C was evaluated. It was assumed that a continuous heating system stabilized temperature at a selected level of 11 °C, ensuring some level of thermal comfort. New lower RH values generated by heating the mass of water vapour in the air, expressed as the humidity mixing ratio, were calculated using the formula proposed by Camuffo [37]. Then, the influence of the simulated temperature and RH conditions on the G_I values was evaluated (Fig. 12). As one can see, RH dropped shortly to 30% during January but the calculated G_I value is still below the critical G_{Ic} level. Similarly to the case of the real climate in the basilica discussed earlier, the reason for the observation is the much slower drying of the sculpture at 11 °C due to a lower diffusion coefficient than is the case during a warm period when the temperature is above 20 °C. Secondly, the drops in RH were significantly shorter than the one recorded on June 23. The effect is also supported by much shallower drying of the sculpture illustrated by the maximal G_I value obtained for crack depths of 5 and 10 mm. It was further found that 11 °C is the highest temperature to which the interior can be continuously heated without causing risk to the sculptures.

Another scenario studied involved moving the sculpture to the conservation studio of perfectly controlled RH. The scenario was simulated by a step change of RH with various amplitudes from the equilibrium conditions of 59% RH for the wide selection of crack depths and temperature of 21 °C. The results are depicted in Fig. 13 where G_{Imax} is the highest value of G_I reached during one year.

The minimal drop in RH that generated propagation of the crack was found to be only 6% for a 100 mm deep crack. It might be surprising that the natural environment with RH varying between 40 and 75% induces lower risk to the sculpture than moving the object from that unstable environment to stable museum conditions considered ideal. However, for existing deep cracks, the time for the drying front to reach their tips is significantly longer than for the shallow cracks as presented in our first methodological paper [6] and in Fig. 14. Consequently, for 100 mm deep crack, the time necessary to reach G_{Ic} after the RH drop from 59 to 53% is 9 months.

The third scenario studied analysed the impact of short-term climate variations related to cultural or religious events. The question about the critical event duration that is safe for the objects studied is particularly relevant. Heating episodes in the church of Santa Maria

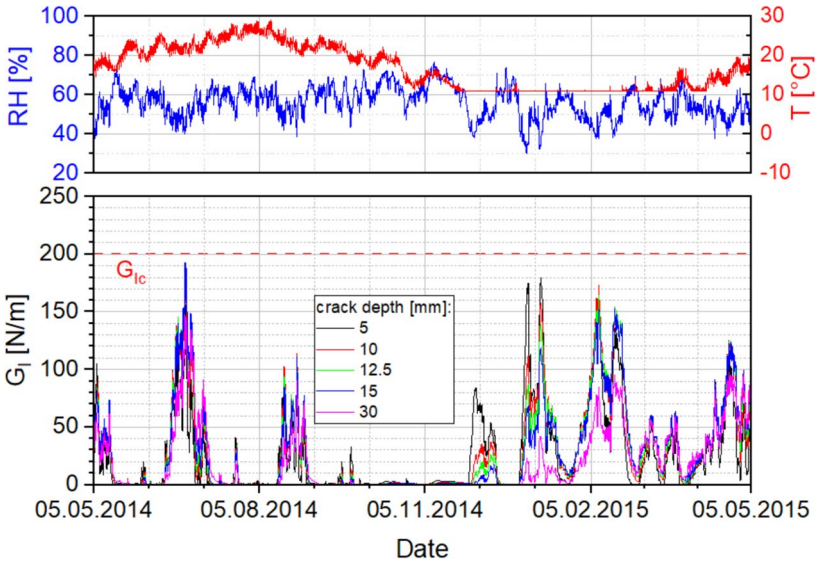

Fig. 12 Effect of the simulated microclimate with continuous heating, set to maintain 11 °C, on the G_I values in the sculpture modelled

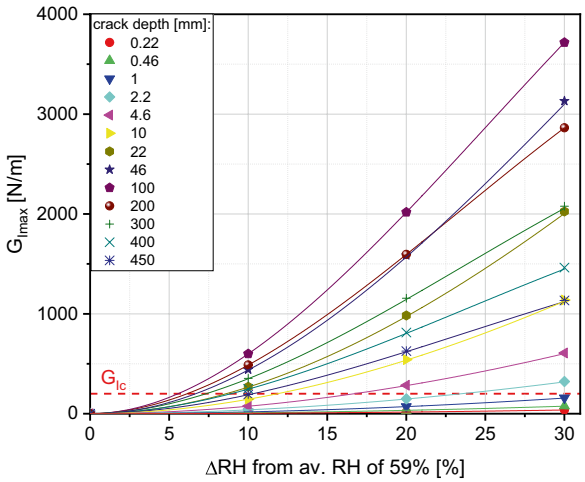

Fig. 13 G_{Imax} reached during one year as a function of a magnitude of an RH drop from 59%

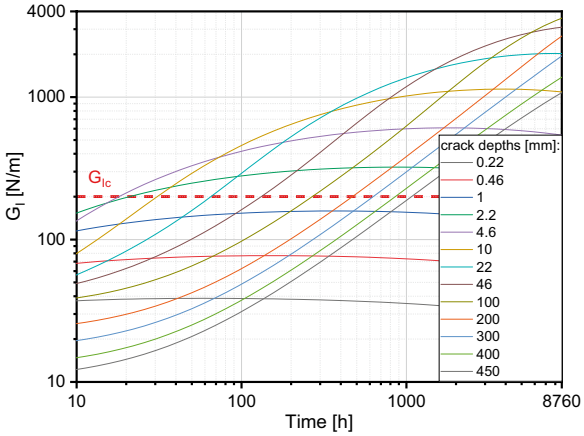

Fig. 14 Evolution of G_I in time for an RH change from 59 to 29%

Maddalena in Rocca Pietore, Italy, heated for two services in December 2002 as shown in Fig. 15 are an example of such events [38]. During the events, temperature rose above 20 °C and RH dropped almost to 30% from the level of 65%.

Increases of G_I induced by a step change of RH from 59 to 20% at a temperature of 18 °C are shown in Fig. 16 for increasing duration of the low RH condition. Such significant RH drops due to heating can happen only during frosty days and can be considered the worst case. It was found that RH drops caused by heating of the interior to thermal comfort conditions, that are shorter than 12 h, will not induce further crack growth, and thus are safe for the massive wooden sculptures. This heating time deemed safe for the sculptures is significantly lower than 60 h determined in [6]. The reason for this is the larger magnitude of the RH drop—almost 40% instead of 30%, and the much larger diameter of the sculpture. As explained in [6], the approach based on the assumption of ideally elastic wood behaviour adopted in the modelling predicts well the initiation of crack growth which has been the focus of this study. However, it should be born in mind that the model is not sufficient to represent the crack propagation in the time domain.

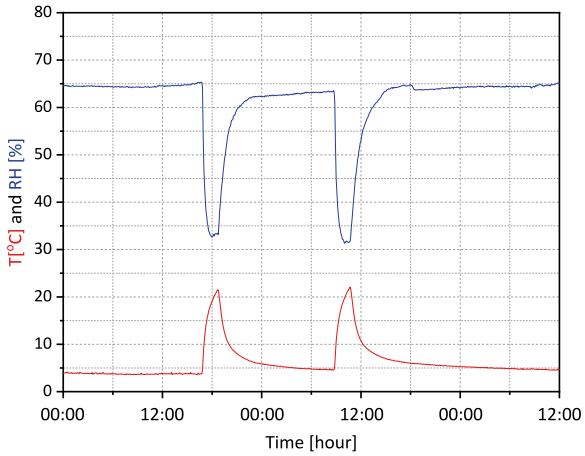

Fig. 15 Temperature and RH during heating episodes in the church of Santa Maria Maddalena, Rocca Pietore [38]

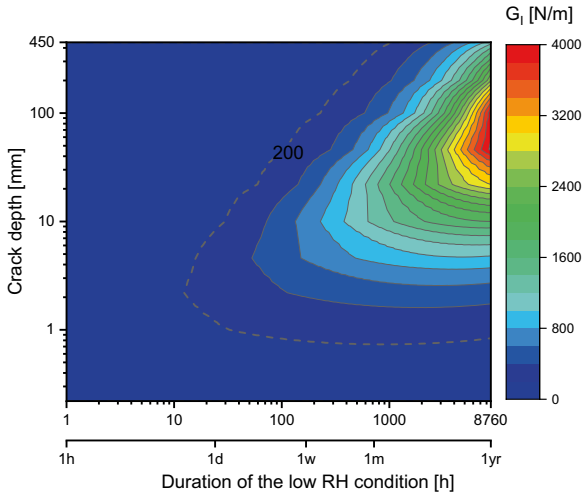

Fig. 16 Two-parameter risk map for an RH change from 59 to 20% at a temperature of 18 °C

Conclusions

The paper has contributed to filling a gap of knowledge on mechanical parameters of a culturally relevant wood species—the lime wood – that are necessary to analyse the risk of crack propagation in sculptures induced by environmental instabilities.

Experimentally determined tensile properties were provided: moduli of elasticity, Poisson's ratios, and strains at break in two anatomical directions, tangential and radial, as well as fracture energy, at four RH levels. Fracture energy was found to increase with RH, therefore, the risk of crack propagation is most significant in dry conditions. The lowest G_f value determined in this study was 350 N/m at RH = 45% which is less than G_f determined for other hardwoods in the TR crack propagation system at RH = 30% given in [27]. It was used to estimate the critical fracture toughness G_{Ic} as 200 N/m which served as the fracture propagation criterion in lime wood.

It was demonstrated that the numerical model of a massive wooden sculpture using the approach of fracture mechanics with experimentally determined material properties can be successfully used to evaluate the risk of cracking engendered by environmental variations recorded in a historical church. The modelling of sculptures from the Veit Stoss' altarpiece revealed that the natural unstable microclimate of the church, recorded over one full year, brought no risk of further fracture to the sculptures. This agreed with the condition survey carried out by the conservation team. It was also estimated that heating the church to a stable level of no more than 11 °C to improve the thermal comfort of the visitors during the cold period would cause decreases in RH to a level that is still safe for the massive sculptures. In the case of St. Mary's Basilica, the maximum drop of RH caused by the hypothetical occasional short-term heating for events like concerts or religious services was assessed to be approximately 40%. The associated risk of crack propagation in sculpture was found to be significant only if the low RH level lasted longer than 12 h. For smaller RH drops the allowable time would be longer. The simulation of the transfer of the sculpture from its natural environment to the conservation studio indicated that the critical G_f value would be reached for an RH drop of only 6% from the equilibrium condition of 59%. The simulation allowed thus the lowest allowable RH level of 54% in the studio to be determined that would be safe for the object.

Abbreviations

a	Hygroscopic dimensional change
D	Diffusion coefficient
EMC	Equilibrium moisture content
G (G_I)	Energy release rate (in mode I)
G_c (G_{Ic})	Critical energy release rate (in mode I)
G_f	Fracture energy
h'	External mass transfer coefficient
MC	Moisture content
RH	Relative humidity
TR	Tangential-radial fracture plane in wood
UTM	Universal testing machine

Supplementary Information

The online version contains supplementary material available at https://doi.org/10.1186/s40494-024-01325-y.

Supplementary Material 1.

Acknowledgements

The authors are grateful for granting access to the computing infrastructure built in the projects POIG.02.03.00-00-028/08 "PLATON—Science Services Platform" and POIG.02.03.00-00-110/13 "Deploying high-availability, critical services in Metropolitan Area Networks (MAN-HA)". They would also like to express their gratitude to Aleksandra Hola from the Academy of Fine Arts in

Kraków for providing seasoned lime wood for mechanical testing. The authors thank Paweł Kozakiewicz and Andrzej Mazur from Warsaw University of Life Sciences – SGGW for their assistance in the machining of the specimens and valuable insights regarding the wedge-splitting experiment.

Author contributions
LB: Conceptualization and development of methodology, analysis and interpretation of the results, and preparation of the manuscript. MS: Development and validation of the model, performing experiments and calculations, data analysis and interpretation, and preparation of the manuscript.

Funding
This work received funding through PRELUDIUM 19 project no. 2020/37/N/HS2/01727 granted by the National Science Centre, Poland, and the statutory research fund of the Jerzy Haber Institute of Catalysis and Surface Chemistry, Polish Academy of Sciences.

Availability of data and materials
All data needed to evaluate the conclusions in the paper are presented in the paper. Additional data related to this paper may be requested from the corresponding author.

Declarations

Competing interests
The authors declare that they have no competing financial interests or personal relationships that could have appeared to influence the work reported in this paper.

Received: 6 April 2024 Accepted: 12 June 2024
Published online: 25 June 2024

References

1. Luimes RA, Suiker ASJ. Numerical modelling of climate-induced fracture and deformation in wood: application to historical museum objects. Int J Solids Struc. 2021;210–211:237–54.
2. Mecklenburg MF. Determining the acceptable ranges of RH and T in museums and galleries, Part 1. A report of the Museum Conservation Institute, the Smithsonian Institution, 2007. https://repository.si.edu/handle/10088/7056.
3. Mecklenburg MF. Determining the acceptable ranges of RH and T in museums and galleries, Part 2. A report of the Museum Conservation Institute, the Smithsonian Institution, 2007. https://repository.si.edu/handle/10088/7055
4. Bratasz Ł. Allowable microclimatic variations for painted wood. Stud Conserv. 2013;58:65–79.
5. Glass SV, Zelinka SL. Moisture relations and physical properties of wood. In: Wood handbook—Wood as an engineering material. U.S. Dept. of Agriculture, Forest Service, Forest Products Laboratory, Madison; 2010. p. 4–1–4–19.
6. Soboń M, Bratasz Ł. A method for risk of fracture analysis in massive wooden cultural heritage objects due to dynamic environmental variations. Eur J Wood Wood Prod. 2022;80:1201–13.
7. Mecklenburg MF, Tumosa CS. An introduction into the mechanical behavior of paintings subjected to changes in temperature and relative humidity. In: Art in transit: studies in the transport of paintings. Washington: National Gallery of Art; 1991. p. 173–214.
8. Mecklenburg MF, Tumosa CS, Erhardt D. Structural response of painted wood surfaces to changes in ambient relative humidity. In: Painted wood: history and conservation. The Getty Conservation Institute, Los Angeles; 1998. p. 464–83.
9. Rachwał B, Bratasz Ł, Łukomski M, Kozłowski R. Response of wood supports in panel paintings subjected to changing climate conditions. Strain. 2012;48:366–74.
10. ASHRAE: Museums, Galleries, Archives and Libraries. ASHRAE Handbook. Chap 24. American Society of Heating and Air-Conditioning Engineers, Atlanta, 2019.
11. Allegretti O, Raffaelli F. Barrier effect to water vapour of early European painting materials on wood panels. Stud Conserv. 2008;53:187–97.
12. Jakieła S, Bratasz Ł, Kozłowski R. Numerical modelling of moisture movement and related stress field in lime wood subjected to changing climate conditions. Wood Sci Technol. 2008;42:21–37.
13. Porter AW. On the mechanics of fracture in wood. For Prod J. 1964;14(2):325–31.
14. Rice JR. A path independent integral and the approximate analysis of strain concentration by notches and cracks. J Appl Mech. 1968;35:379–86.
15. Yeh B, Schniewind AP. Elasto-plastic fracture mechanics of wood using the J-integral method. Wood Fiber Sci. 1992;24(3):364–76.
16. Gebhardt C, Kaliske M. An XFEM-approach to model brittle failure of wood. Eng Struct. 2020;212: 110236.
17. Chen K, Qiu H, Sun M, Lam F. Experimental and numerical study of moisture distribution and shrinkage crack propagation in cross section of timber members. Constr Build Mater. 2019;221:219–31.
18. Phan NA. Simulation of time-dependent crack propagation in a quasi-brittle material under relative humidity variations based on cohesive zone approach: application to wood. Dissertation, Université de Bordeaux. 2016
19. Hamdi SE, Moutou Pitti R, Dubois F. Temperature variation effect on crack growth in orthotropic medium: Finite element formulation for the viscoelastic behavior in thermal cracked wood-based materials. Int J Solids Struc. 2017;115–116:1–13.
20. Hamdi SE, Moutou PR. Numerical investigation of climate change impacts on European wood species vulnerability. Procedia Structural Integrity. 2018;13:523–8.
21. Stanzl-Tschegg SE, Keunecke D, Tschegg EK. Fracture tolerance od reaction wood (yew and spruce wood in the TR crack propagation system). J Mech Behav Biomed Mater. 2011;4:688–98.
22. Stanzl-Tschegg SE, Tan DM, Tschegg EK. New splitting method for wood fracture characterization. Wood Sci Technol. 1995;29:31–50.
23. Luimes RA, Sukier ASJ, Verhoosel CV, Jorissen AJM, Schellen HL. Fracture behaviour of historic and new oak wood. Wood Sci Technol. 2018;52:1243–69.
24. Reiterer A, Tschegg S. The influence of moisture content on the mode I fracture behaviour of sprucewood. J Mater Sci. 2002;37:4487–91.
25. Schachner H, Reiterer A, Stanzl-Tschegg SE. Orthotropic fracture toughness of wood. J Mater Sci. 2000;19:1783–5.
26. Kossakowski PG. Influence of anisotropy on the energy release rate G(i) for highly orthotropic materials. J Theor Appl Mech. 2007;45:739–52.
27. Vasic S, Stanzl-Tschegg S. Experimental and numerical investigation of wood fracture mechanisms at different humidity levels. Holzforschung. 2007;61:367–74.
28. Majka J, Olek W. Sorption properties of mature and juvenile lime wood (Tilia sp.) Folia Forestalia Polonica B 2008;39:65–75.
29. Popescu CM, Hill CA. The water vapour adsorption-desorption behaviour of naturally aged *Tilia cordata* Mill. Wood, Polym Degrad Stab. 2013;98:1804–13.
30. Konopka D, Grohmann B, Gecks J, Scheiding W, Kaliske M. Short-term hygro-mechanical behaviour of lime wood (*Tilia cordata*) in principal anatomical directions. Holzforschung. 2024. https://doi.org/10.1515/hf-2023-0029.
31. Rockland LB. Saturated salt solutions for static control of relative humidity between 5° and 40°C. Anal Chem. 1960;32(10):1375–6.
32. ISO 3346–1975(E) Wood – Determination of ultimate tensile stress perpendicular to grain.
33. Schindelin J, Arganda-Carreras I, Frise E, Kaynig V, Longair M, Pietzsch T, Preibish S, Rueden C, Saalfeld S, Schmid B, Tinevez JY, White DJ, Hartenstein V, Eliceiri K, Tomancak P, Cordona A. Fiji: an open source platform for biological-image analysis. Nat Methods. 2012;9:676–82.
34. Bratasz Ł, Kozłowska A, Kozłowski R. Analysis of water adsorption by wood using the Guggenheim-Anderson-de Boer equation. Eur J Wood Prod. 2012;70:445–51.
35. Mualem Y. A conceptual model of hysteresis. Water Resour Res. 1974;10:514–20.
36. Bratasz Ł, Kozłowski R, Kozłowska A, Rachwał B. Sorption of moisture and dimensional change of wood species used in historic objects. In: Gril J,

editor. Wood science for conservation of cultural heritage—Braga 2008: proceedings of the international conference held by COST Action IE0601. Firenze University Press: Florence; 2010. p. 11–6.
37. Camuffo D. Microclimate for cultural heritage. Developments in atmospheric science 23. 2nd ed. Elsevier; 2013.
38. Bratasz Ł, Kozłowski R. Laser sensors for continuous in-Situ monitoring of the dimensional response of wooden objects. Stud Conserv. 2005;50:307–15.

Publisher's Note